Comprehensive analysis of lymph node stroma-expressed Ig superfamily members reveals redundant and nonredundant roles for ICAM-1, ICAM-2, and VCAM-1 in lymphocyte homing

Rémy T. Boscacci,[1] Friederike Pfeiffer,[1] Kathrin Gollmer,[1] Ana Isabel Checa Sevilla,[2] Ana Maria Martin,[2] Silvia Fernandez Soriano,[1] Daniela Natale,[1] Sarah Henrickson,[3] Ulrich H. von Andrian,[3] Yoshinori Fukui,[4,5] Mario Mellado,[2] Urban Deutsch,[1] Britta Engelhardt,[1] and Jens V. Stein[1]

[1]Theodor Kocher Institute, University of Bern, Bern, Switzerland; [2]National Center for Biotechnology, Spanish Research Council, Campus de Cantoblanco, Madrid, Spain; [3]Department of Pathology, Harvard Medical School, Boston, MA; [4]Division of Immunogenetics, Department of Immunobiology and Neuroscience, Medical Institute of Bioregulation, Kyushu University, Fukuoka, Japan; and [5]Japan Science and Technology, Core Research for Evolutional Science and Technology (CREST), Tokyo, Japan

Although it is well established that stromal intercellular adhesion molecule-1 (ICAM-1), ICAM-2, and vascular cell adhesion molecule-1 (VCAM-1) mediate lymphocyte recruitment into peripheral lymph nodes (PLNs), their precise contributions to the individual steps of the lymphocyte homing cascade are not known. Here, we provide in vivo evidence for a selective function for ICAM-1 > ICAM-2 > VCAM-1 in lymphocyte arrest within noninflamed PLN microvessels. Blocking all 3 CAMs completely inhibited lymphocyte adhesion within PLN high endothelial venules (HEVs). Postarrest extravasation of T cells was a 3-step process, with optional ICAM-1–dependent intraluminal crawling followed by rapid ICAM-1– or ICAM-2–independent diapedesis and perivascular trapping. Parenchymal motility of lymphocytes was modestly reduced in the absence of ICAM-1, while ICAM-2 and α4-integrin ligands were not required for B-cell motility within follicles. Our findings highlight nonredundant functions for stromal Ig family CAMs in shear-resistant lymphocyte adhesion in steady-state HEVs, a unique role for ICAM-1 in intraluminal lymphocyte crawling but redundant roles for ICAM-1 and ICAM-2 in lymphocyte diapedesis and interstitial motility. (*Blood*. 2010;116(6):915-925)

Introduction

To ensure rapid encounters between Ag and rare lymphocytes, strategically positioned secondary lymphoid organs (SLOs) filter, retain, and present Ag to passing lymphocytes.[1] In case lymphocytes do not encounter their specific Ag on antigen-presenting cells (APCs), they exit SLOs after approximately 8 to 12 hours and reenter the blood stream via efferent lymphatics.[2] As an adaptation to their motile lifestyle, lymphocytes undergo transient adhesive interactions with other hematopoietic and stromal cells. Lymphocytes interact mainly with 2 types of stromal cells: First, blood-borne lymphocytes adhere to endothelial cells, in particular those composing the high endothelial venules (HEVs) of peripheral lymph nodes (PLNs) and other lymphoid tissues.[2,3] Second, T and B cells move along fibroblast-like cells forming the stromal network underlying the 3-dimensional matrix of lymphoid microenvironments, that is, the follicular dendritic cells (FDCs) of B-cell follicles, the T-cell zone fibroblastic reticular cells (TRCs) and marginal reticular cells (MRCs) in the cortex of B-cell follicles and interfollicular areas.[4-6]

These transient stroma-lymphocyte interactions are central to immunosurveillance and have thus been examined in previous studies, in particular using genetically modified or inhibitor-treated lymphocytes. The molecular mechanisms governing the rapid firm adhesion of blood-borne lymphocytes within PLN HEVs follow a multistep adhesion sequence, where CD62L-mediated tethering and rolling on peripheral lymph node addressin (PNAd) expressed on HEVs is followed by activation of the chemokine receptor CCR7 on rolling lymphocytes. This is because HEVs present the CCR7 ligands CCL19 and, in particular, CCL21 on their luminal surface.[7,8] CCR7 activation and shear forces from the continuous blood flow lead to a rapid conformational activation of LFA-1 leading to increased affinity for adhesion receptors of the intercellular adhesion molecule (ICAM) superfamily, in particular ICAM-1 and ICAM-2.[9] Furthermore, chemokine-activated α4 integrins can bind vascular cell adhesion molecule-1 (VCAM-1) and mucosal addressin cell adhesion molecule-1 (MAdCAM-1). Rapid integrin activation results in a sudden stop of lymphocytes rolling in HEVs.[10,11] The molecular mechanisms involved in the subsequent transendothelial migration (TEM) of firmly adherent lymphocytes across HEVs into the surrounding lymphoid tissue are less well understood, although in vitro studies suggest the formation of specialized docking/capping structures between endothelial cells and lymphocytes. In particular, ICAM-1 and VCAM-1 form circular structures surrounding adherent lymphocytes, which are thought to facilitate adhesion and trans- or paracellular lymphocyte crossing of the endothelial lining.[12-14] After transmigration, twophoton microscopy (2PM) experiments have shown that T cells move along TRCs, which express ICAM-1.[6,15] Lack of ICAM-1 on stromal cells resulted in a minor decrease in T-cell motility, in line with a migration mode mostly driven by the Rac

Submitted November 13, 2009; accepted April 7, 2010. Prepublished online as *Blood* First Edition paper, April 15, 2010; DOI 10.1182/blood-2009-11-254334.

The online version of this article contains a data supplement.

The publication costs of this article were defrayed in part by page charge payment. Therefore, and solely to indicate this fact, this article is hereby marked "advertisement" in accordance with 18 USC section 1734.

guanine exchange factor (GEF) dedicator of cytokinesis protein 2 (DOCK2) and Rac-dependent lamellipodia formation.[16-18]

Despite recent in vitro observations, the precise roles for Ig superfamily members during individual steps of in vivo lymphocyte trafficking to PLNs—arrest and crawling on the HEVs, TEM across the HEVs and parenchymal motility—have not been examined thus far. Whereas ICAM-1 is expressed at low levels in most endothelial beds and is only increased during inflammation, it is constitutively expressed at high levels on HEVs.[19,20] ICAM-2 is constitutively expressed in most vascular beds including HEVs.[21] Although ICAM-1 and ICAM-2 have been shown to be involved in lymphocyte homing to PLNs,[22] their precise contribution to lymphocyte arrest and crawling on the HEV versus lymphocyte diapedesis has not been investigated. Furthermore, a role for α4 integrins during lymphocyte homing into PLNs remains controversial.[10,23] ICAM-1, VCAM-1 and MAdCAM-1 are also highly expressed on MRCs and/or FDCs,[5,6,24] thus potentially contributing to interstitial B-cell motility. This may be particularly relevant because B cells are more dependent on ICAM-1 and VCAM-1 expression for successful migration into the splenic white pulp than T cells,[25] and because B cells express high levels of α4 integrins, which can mediate lymphocyte crawling in vitro.[26] Nonetheless, the role for CAMs during parenchymal B-cell migration has not been examined to date.

To address how and which stromal Ig CAM members contribute to adhesive interactions between lymphocytes and the lymphoid tissue microenvironment, we systematically investigated the roles of stromal ICAM-1, ICAM-2 and α4 integrin ligands during all steps of lymphocyte recirculation, from shear-resistant arrest to intraluminal crawling on HEVs, transmigration across the HEV and parenchymal motility within the PLN, using intravital imaging and 3-dimensional (3D) tissue reconstructions. Our findings support a model where ICAM-1 and -2 are required for most shear-resistant lymphocyte adhesion in HEVs, whereas transmigration and parenchymal motility still occur in the absence of either one or both molecules.

Methods

Antibodies and reagents

All monoclonal antibodies (mAbs) were purchased from BD Pharmingen unless otherwise indicated. For generation of mAb-conjugated quantum dots, see supplemental Methods (available on the *Blood* Web site; see the Supplemental Materials link at the top of the online article).

Mice

Male and female C57BL/6 mice were purchased from Harlan (Netherlands). ICAM-1$^{-/-}$ and ICAM-2$^{-/-}$ mice were previously described[27-29] and backcrossed onto the C57BL/6 background for at least 8 generations. ICAM-1/ICAM-2-double deficient (ICAM-1/2$^{-/-}$) C57BL/6 mice were obtained by mating ICAM-1$^{-/-}$ and ICAM-2$^{-/-}$ C57BL/6 mice. Mice were bred in the central animal facility of the Department for Clinical Research of the University of Bern. All animal procedures were performed in accordance with the Swiss legislation on the protection of animals and approved by the veterinary office of the Kanton of Bern.

Intravital microscopy of inguinal PLNs

The left subiliac PLN of male and female 5 to 8-week-old C57BL/6 mice was essentially prepared as described previously.[30] For more details and analysis, see supplemental Methods.

Short-term in vivo homing experiments

Short-term homing of fluorescently labeled T cells was carried out as described,[18] with some modifications. For a detailed description, see supplemental Methods.

3D quantitative immunofluorescence

Fluorescently labeled lymphocytes were injected intravenously into wild-type (WT) recipient mice and allowed to home for 30 minutes before blocking further homing with anti–L-selectin mAb. After 30 minutes, PLNs were isolated, dehydrated in MeOH and transferred to a mixture of benzyl alcohol and benzyl benzoate (BABB) for tissue clearing. BABB-treated PLNs were then analyzed using a twophoton laser scanning microscopy (2PM) setup (LaVision Biotec). For a detailed description, see supplemental Methods.

2PM of popliteal PLNs

The popliteal lymph node of anesthetized mice was essentially prepared as described.[31] Live 2PM was performed with an Olympus BX50WI fluorescence microscope equipped with a 20× NA objective and a TrimScope 2PM system controlled by Imspector software (LaVision Biotec). The track velocity is the average cellular velocity between start and end of track, the instantaneous 3D velocity is the velocity between 2 frames, and the turning angle describes the angle between the 2 velocity vectors before and after a measurement time point. The meandering index (MI) is calculated as the ratio of the distance between start and end point of an individual track and the total track distance. For more details and analysis, see supplemental Methods.

Statistical analysis

Data are presented as mean plus or minus SEM unless otherwise indicated. For comparison of sticking fractions before and after mAb treatment in identical venules, a paired Student *t* test was used. For comparison of sticking fractions of transferred cells in different venules, a nonparametric Mann-Whitney test or Kruskall-Wallis test was performed. For simultaneous comparison of the sticking fractions in venules of different mouse strains, a Dunn multiple comparison test was used. Student *t* tests and analysis of variance were used for 2PM analysis. Statistical significance was set at P less than .05.

Results

Reduced homeostatic lymphocyte numbers in ICAM-1/ICAM-2-deficient PLNs

To analyze the roles of ICAM-1 and ICAM-2 during lymphocyte trafficking, we generated ICAM-1 x ICAM-2-double deficient mice (ICAM-1/2$^{-/-}$). While WT PLNs showed high endothelial expression of ICAM-1 and ICAM-2, and variable expression levels in the parenchyma and in cortical regions, no expression of ICAM-1 and ICAM-2 was detected in ICAM-1/2$^{-/-}$ PLN sections (Figure 1A). We found no obvious alterations in PLN size and structure of either ICAM-1$^{-/-}$ or ICAM-2$^{-/-}$ single-deficient PLNs as described before[27,28] (data not shown). In contrast, ICAM-1/2$^{-/-}$ PLNs were visibly smaller than WT PLNs. The overall structural organization with a clear separation of the lymphoid parenchyma into B-cell follicles and T-cell areas was preserved in the absence of ICAM-1 and ICAM-2 (Figure 1Ai and 1Avi). Similarly, the parenchymal laminin^{+} network and basement membrane around blood vessels were comparable in ICAM-1/2$^{-/-}$ and WT PLNs (Figure 1Aii-v,vii-viii).

In line with the reduced lymphoid organ size, total lymphocyte numbers were reduced 6-fold in ICAM-1/2$^{-/-}$ PLNs (Figure 1B), whereas lymphocyte numbers from mesenteric lymph nodes (MLNs) and Peyer patches (PPs) were only 2-fold decreased (Figure 1C-D).

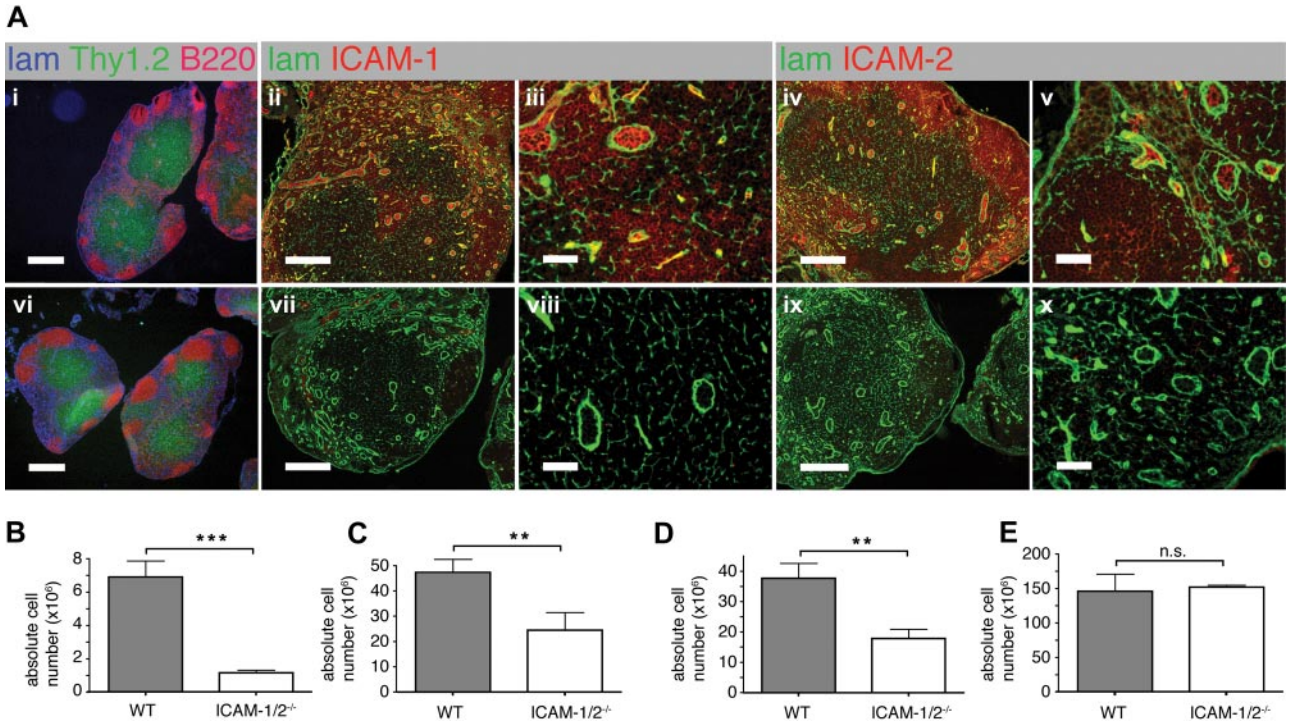

Figure 1. PLN architecture and cellularity of lymphoid organs in WT and ICAM-1/2$^{-/-}$ mice. (A) Immunofluorescent staining of PLN sections of WT (i-v) and ICAM-1/2$^{-/-}$ (vi-x) mice. i,vi: laminin (lam; blue), Thy1.2 (green), and B220 (red). Scale bar = 400 μm. ii,iii,vii,viii: laminin (lam; green) and ICAM-1 (red). Scale bar = 200 μm (ii,vii) or 40 μm (iii,viii). iv,v,ix,x: laminin (lam; green) and ICAM-2 (red). Scale bar = 200 μm (iv,ix) or 40 μm (v,x). (B-E) Absolute cell numbers per cervical, brachial, axillary, inguinal, paraaortal, and popliteal PLNs (B), MLN (C), PP (D), and spleen (E) of WT and ICAM-1/2$^{-/-}$ mice, represented as mean plus or minus SEM pooled from 3 (PLN, MLN, spleen) or 4 (PP) independent experiments. n.s. indicates not significant. $^{**}P < .01$; $^{***}P < .0001$.

Splenocyte numbers were comparable in WT and ICAM-1/2$^{-/-}$ mice (Figure 1E and supplemental Figure 1). Similarly, thymocyte numbers and CD4$^+$, CD8$^+$ single/double rations in the absence of ICAM-1 and ICAM-2 were similar to WT thymi (data not shown). We next performed a flow cytometric analysis of the lymphocyte subsets in WT and ICAM-1/2$^{-/-}$ PLNs. We were unable to detect significant differences in the percentages of CD4$^+$, CD8$^+$, and B220$^+$ cells, as well as CD62L, CD44, CD25, LFA-1 or α4 integrin cell surface levels (supplemental Figure 1). In summary, the dual lack of ICAM-1 and ICAM-2 resulted in a strong decrease in PLN cellularity, while mucosal secondary lymphoid organs were less affected.

Preferential use of endothelial ICAM-1 over ICAM-2 for lymphocyte arrest in the PLN microvasculature

The phenotype of the ICAM-1/2$^{-/-}$ mice suggested deregulated lymphocyte trafficking to and/or within PLNs. Because lymphocyte trafficking involves adhesion in HEVs, TEM across the HEV and interstitial motility, we set out to investigate the roles of ICAM-1 and ICAM-2 in the individual steps of the lymphocyte homing process. First, we addressed the contribution of ICAM-1 and ICAM-2 during the multistep adhesion of circulating naive lymphocytes on HEVs of PLNs using intravital microscopy (IVM). In a first set of experiments, we injected fluorescently labeled WT lymphocytes into anesthetized mice surgically prepared to expose the inguinal PLN microarchitecture, in the presence or absence of blocking mAbs against ICAM-1 or ICAM-2. As predicted from previous studies using anti–LFA-1 mAbs,[10] lymphocyte tethering and rolling was most efficient in small HEVs and not affected by inhibition of ICAM-1 or ICAM-2 (Figure 2A). In contrast, we observed a significant 3-fold reduction in the fraction of cells arrested for more than 20 seconds, the so-called sticking fraction, in the presence of blocking mAbs against ICAM-1, but not ICAM-2 (Figure 2A-B). Blocking ICAM-1 resulted in a transient reduction of lymphocyte arrest in HEVs, because lymphocytes were found to successfully attach to PLN HEVs at later time points (> 30 minutes) of the analysis (data not shown).

We next analyzed the rolling and shear-resistant arrest of fluorescently labeled naive lymphocytes in the PLN microvasculature of control and ICAM-1$^{-/-}$, ICAM-2$^{-/-}$ and ICAM-1/2$^{-/-}$ mice. ICAM-1$^{-/-}$ PLN stromal cells showed comparable ICAM-2 surface levels as WT PLNs, and vice versa (supplemental Figure 2). Similar to the Ab-blocking experiments, the rolling fractions were not altered in the absence of ICAM-1 and/or ICAM-2 (Figure 2C). Absence of ICAM-1, but not ICAM-2, led to a 3-fold reduction in the lymphocyte sticking fraction compared with WT mice; after prolonged observation (> 30 minutes), ICAM-1-independent lymphocyte accumulation could nonetheless be detected (data not shown). Administration of anti–ICAM-2 mAbs resulted in a further significant (35% ± 10%, mean ± SEM) reduction of lymphocyte arrest in ICAM-1$^{-/-}$ venules, indicating that endothelial ICAM-2 can partially compensate for the lack of ICAM-1 (Figure 2D). Accordingly, the sticking fraction of naive lymphocytes was reduced by 87% (± 35%) in ICAM-1/2 $^{-/-}$ mice compared with WT mice (supplemental Videos 1-2). The low number of residual firmly adherent lymphocytes detected in ICAM-1/2$^{-/-}$ HEVs precluded a meaningful analysis of the alternative adhesion pathways using IVM (data not shown).

In conclusion, our data show that endothelial ICAM-1 plays a predominant role in shear-resistant arrest of naive lymphocytes in the PLN microvasculature. Importantly, the observed reduction of lymphocyte arrest in the absence of functional ICAM-1 delayed lymphocyte accumulation in PLN HEVs only

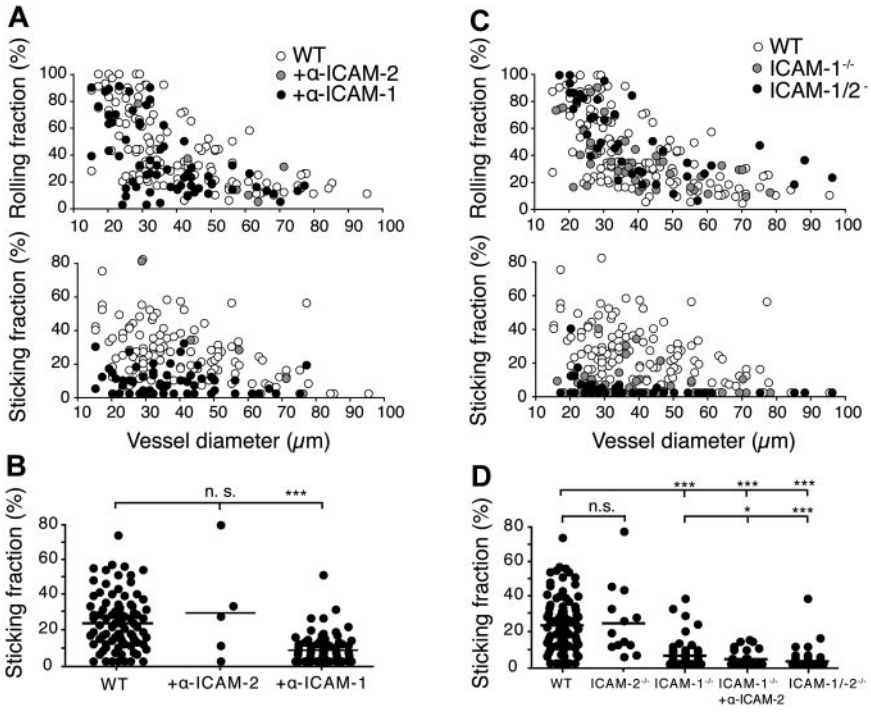

Figure 2. IVM analysis of lymphocyte rolling and shear-resistant firm adhesion in mAb-blocked WT and ICAM-1$^{-/-}$, ICAM2$^{-/-}$ and ICAM-1/2$^{-/-}$ PLN microvasculature. (A) Rolling (top panel) and sticking fractions (bottom panel) of lymphocytes in WT PLN microvessels as a function of vessel diameter and in the presence of blocking antibodies against ICAM-1 or ICAM-2. Each dot represents 1 venule. Pooled from 3 (+anti–ICAM-2), 18 (+anti–ICAM-1), and 27 (no Abs) WT animals per condition with 5 (+anti–ICAM-2), 59 (+anti–ICAM-1) and 126 (no Abs) venules analyzed. (B) Sticking fractions of lymphocytes in WT PLN microvessels as in panel A. Each dot represents 1 venule. Bars represent mean values. n.s. indicates not significant. ***$P < .0001$. (C) Rolling (top panel) and sticking fractions (bottom panel) of lymphocytes in WT, ICAM-1$^{-/-}$, and ICAM-1/2$^{-/-}$ PLN microvessels as a function of vessel diameter. Each dot represents 1 venule. Pooled from 6 ICAM-1$^{-/-}$, 6 ICAM-1/2$^{-/-}$, and 27 WT animals with 45 (ICAM-1$^{-/-}$), 42 (ICAM-1/2$^{-/-}$), and 126 (WT) venules analyzed. (D) Sticking fractions of lymphocytes in WT, ICAM-2$^{-/-}$ (4 animals, 13 venules analyzed), ICAM-1$^{-/-}$, ICAM-1$^{-/-}$ + anti–ICAM-2 (4 animals, 29 venules analyzed) and ICAM-1/2$^{-/-}$ PLN microvessels as in panel C. Each dot represents 1 venule. Numbers of WT, ICAM-1$^{-/-}$, and ICAM-1/2$^{-/-}$ animals and analyzed venules as in panel C. Bars represent mean values. n.s. indicates not significant. *$P < .05$; ***$P < .0001$.

during a short time window, presumably because recirculating lymphocytes eventually adhere through ICAM-2-dependent mechanisms. In addition, our findings suggest the presence of a minor, ICAM-1/2-independent lymphocyte adhesion pathway in a subset of small PLN HEVs.

Dynamic imaging of lymphocyte egress from HEVs

We next set out to use 2PM to examine the precise dynamics of lymphocyte transmigration across HEVs and the role for ICAM-1 and other CAMs in this process. To identify HEVs and blood lumen, we i.v. injected Alexa633- or quantum dot (QD) 655-conjugated MECA79 as specific anatomical landmarks for long-term observation of HEVs, together with a plasma marker, 15 minutes before recording (supplemental Videos 3-8). Fluorescently labeled naive T cells were injected intravenously at the time of onset of the recording and carefully tracked from the site of shear-resistant arrest within HEVs to their appearance within the lymphoid parenchyma. Transferred T cells, which colocalized with MECA-79 and plasma markers were defined as "luminal," while T cells that had crossed the MECA-79$^+$ lining but remained associated with it (< 20 μm distance) were defined as "perivascular." T cells, which were further than 20 μm away from the MECA-79$^+$ endothelial lining, were considered "parenchymal."

The tracking analysis uncovered that approximately two-thirds (68%) of the arrested T cells directly egressed from their site of firm adhesion to the underlying parenchyma (< 20 μm distance migrated; supplemental Video 4). In contrast, approximately one-third (32%) of T cells "crawled" on the high endothelial cells for more than 20 μm until transmigrating across the HEV into the perivascular space, with an average migrated distance of 53.8 (± 7.2) μm (mean ± SEM) and an average intraluminal dwelling time of 7.0 (± 1.0) minutes (Figure 3A-B; supplemental Video 5). Crawling T cells migrated along, against, or perpendicular to the direction of the blood flow (J.V.S., unpublished observations, 2009) and were characterized by a polarized shape, with an average migration velocity of 8.5 (± 0.6) μm/min (Figure 3B).

Irrespective of whether T cells were crawling or directly egressing, the actual "transmigration event," that is, crossing of the MECA-79$^+$ endothelial lining, was typically fast, with durations of 30 to 150 seconds between intraluminal and perivascular localization of individual T cells (Figure 3A; supplemental Videos 4-5). Transmigration was also often accompanied by significant shape changes of crossing T cells, with a thin protrusion followed by the quick translocation of the entire T-cell body (J.V.S., unpublished observations, 2009). After transmigration, we mostly observed a delay in further directed motility and low directional persistence, indicative of "perivascular trapping" around HEVs (Figure 3A,C). Perivascular cells typically formed numerous protrusions, indicative of an active probing behavior (supplemental Videos 4-5). Because HEVs are surrounded by a basement membrane and a cuff of stromal cells, we reasoned that the T-cell passage through the extracellular matrix and the surrounding cells was causing a decrease in velocity and directionality. Consistent with this assumption, perivascular T cells colocalized with laminin around HEVs (Figure 3D). Once T cells had moved approximately 20 μm away from the MECA-79$^+$ lining, we observed a sudden increase of migration velocity. Due to the limited tracking period, these parenchymal T cells showed high directionality and often disappeared rapidly from the field of view (Figure 3C).

During image analysis of transmigrating T cells, we noticed a rapid acquisition of a flattened, polarized cell shape in T cells that adhered inside HEVs. To further explore the molecular basis underlying dynamic lymphocyte transmigration through HEVs, we tracked adherent T cells lacking the actin cytoskeleton regulator DOCK2.[18,32,33] Adherent DOCK2$^{-/-}$ T cells directly egressed from the site of adhesion, yet typically remained trapped in the perivascular location until the end of the recording (supplemental Figure 3; supplemental Videos 6-7). Thus, crawling on endothelium and egress from the perivascular location, but not transmigration itself, depended on DOCK2-Rac-mediated cytoskeletal activity, as observed in vitro.[34]

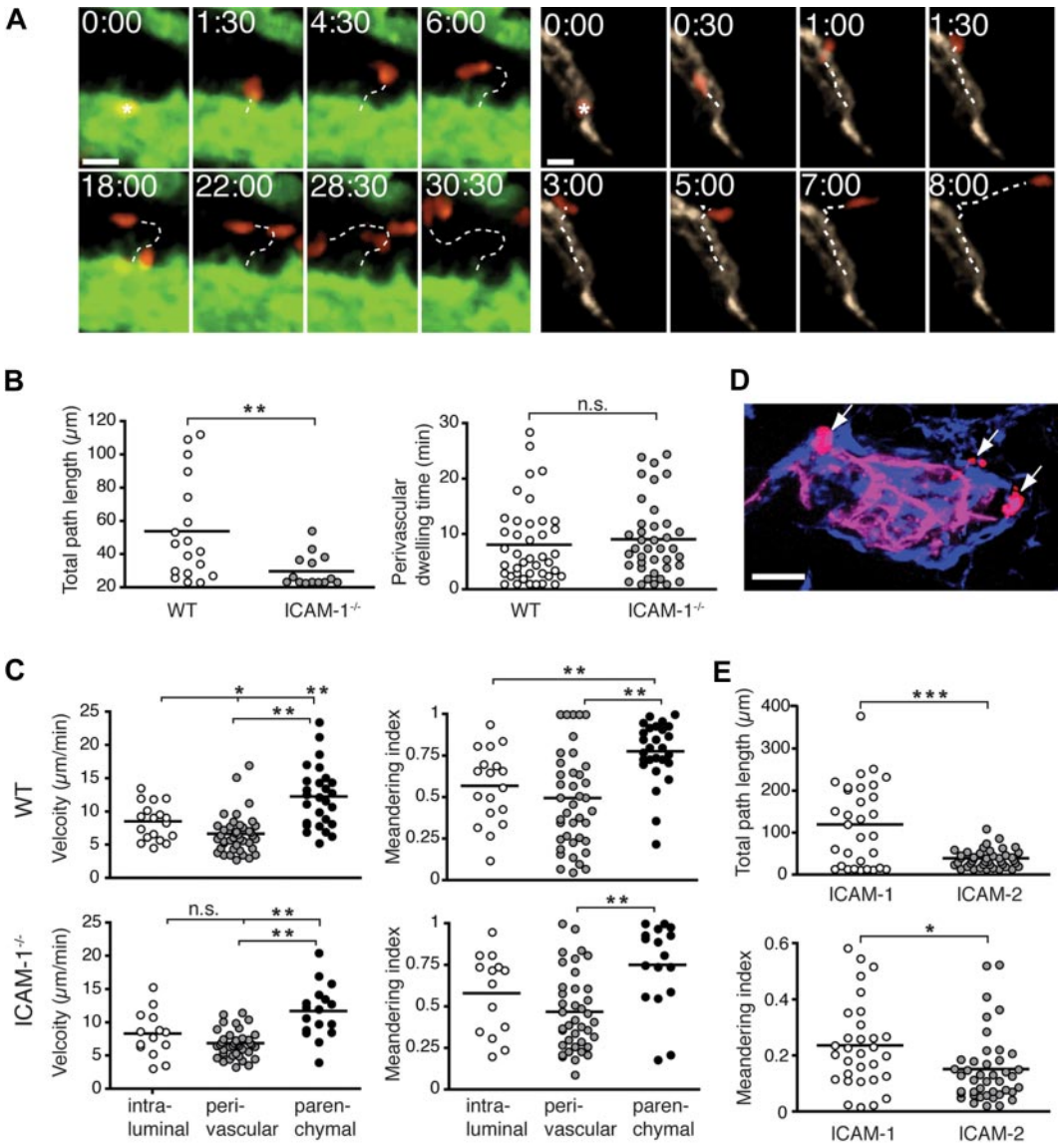

Figure 3. A nonredundant role for ICAM-1 for intraluminal T-cell crawling, but not transendothelial migration or perivascular trapping. (A) Representative micrographs of directly egressing (left panels) or crawling (right panels) T cells transmigrating through HEVs. Time in minutes and seconds; scale bar = 10 μm. (B left panel) Total path length of crawling T cells in WT or ICAM-1$^{-/-}$ PLNs. (Right panel) Perivascular dwelling of transmigrated T cells in WT or ICAM-1$^{-/-}$ PLNs. (C top panels) Mean track velocity (right) and meandering index (MI; left) of crawling intraluminal T cells, as well as perivascular and parenchymal T cells in WT PLNs. The low velocity and MI are indicative of the perivascular slowing down of transmigrated T cells. (Bottom panels) Mean track velocity (right) and MI (left) of intraluminal perivascular and parenchymal T cells in ICAM-1$^{-/-}$ PLNs. (D) Immunofluorescent image of transmigrated T cells (red, arrows) around a MECA-79^{+} HEV (pink) 15 minutes after transfer. Transferred cells are in close proximity to the laminin^{+} basement membrane (blue). Scale bar = 10 μm. (E) Total path length (top panel) and MI (bottom panel) of naive T cells migrating on 2D surfaces coated with CCL21 + ICAM-1/Fc or ICAM-2/Fc. Tracks were recorded for 20 minutes. One experiment of 3 is shown. n.s. indicates not significant. *$P < .05$; **$P < .001$; ***$P < .0001$.

Lymphocyte crawling on HEVs, but not successful transmigration across HEVs, is impaired in the absence of ICAM-1

Having defined the baseline lymphocyte transmigration parameters, we next investigated the contribution of ICAM-1 during this process. We observed efficient T-cell accumulation in ICAM-1$^{-/-}$ PLN HEVs during the time course of the recording (30-45 minutes), which allowed us to track a meaningful number of T cells from their site of arrest to their appearance within the lymph node parenchyma. We found that the time required for adhered intraluminal T cells to cross the MECA-79^{+} lining in the absence of ICAM-1 was comparable with WT PLNs (mean translocation time of directly egressing T cells in WT PLN HEVs: 81 ± 35 seconds; in ICAM-1$^{-/-}$ PLN HEVs: 86 ± 58 seconds; p = 0.66, Mann-Whitney test and supplemental Video 8). Also, approximately one-third (34%) of arrested T cells moved for more than 20 μm on ICAM-1$^{-/-}$ HEVs before transmigration; however, the average distance migrated by these cells was significantly lower than in the presence of ICAM-1 (29.5 ± 2.8 μm; Figure 3B and supplemental Figure 4), indicating that ICAM-1 was required for efficient T-cell crawling on high endothelial cells. Because the endothelial surface distribution of ICAM-1 versus ICAM-2 may also affect cellular behavior, we performed in vitro experiments using purified ICAM-1 or ICAM-2 coimmobilized with CCL19 or CCL21. Similar to our in vivo observations, ICAM-1, but not ICAM-2, supported efficient 2-dimensional (2D) migration of naive T cells (Figure 3E). Comparable results were obtained when CXCL12 was used as promigratory factor (supplemental Figure 5).

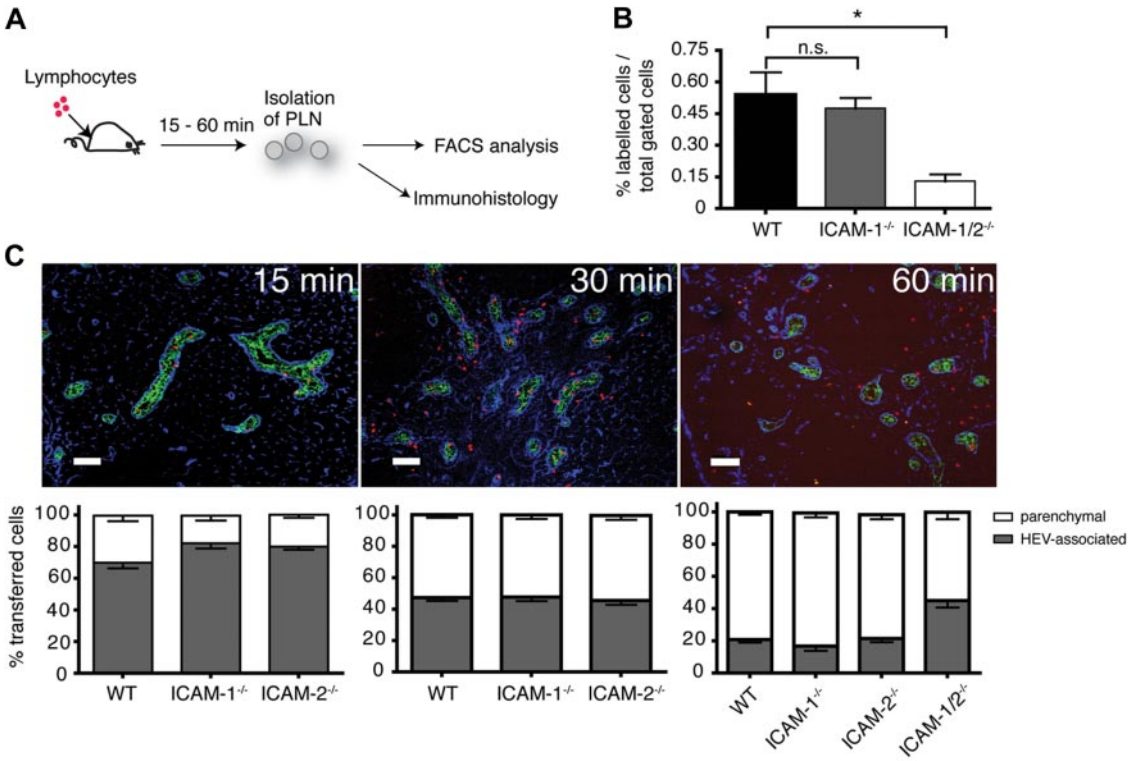

Figure 4. Reduced homing in the absence of ICAM-1 and 2. (A) Schematic outline of short-term homing experiment. Fluorescently labeled lymphocytes were injected and allowed to home for 15, 30, or 60 minutes. PLNs were analyzed by flow cytometry or immunohistology. (B) Flow cytometric analysis of homing efficiency in the absence of ICAM-1 or ICAM-1 and ICAM-2. PLNs were analyzed 60 minutes after cell transfer. The percentage of fluorescently labeled lymphocytes of the total PLN cell population is depicted. Pooled from 4 independent experiments. (C top panel) Immunofluorescent analysis of PLN sections at 15, 30, and 60 minutes after cell transfer. Transferred lymphocytes are labeled in red, HEVs (MECA-79$^+$) in green, and ERTR7 (in the PLN parenchyma and the HEV basement membrane) in blue. Cells within the ERTR7$^+$ ring around HEVs were defined as vessel associated and cells outside as parenchymal. Scale bar = 100 μm. (Bottom panel) Localization of transferred lymphocytes in WT, ICAM-1$^{-/-}$, ICAM-2$^{-/-}$, and ICAM-1/-2$^{-/-}$ PLNs at 15, 30, and 60 minutes after cell transfer. Absolute numbers per section were normalized to 100%. Bars represent mean plus or minus SEM pooled from 3 to 5 independent experiments.

Comparable with WT PLNs, perivascular T cells showed low directional movement around ICAM-1$^{-/-}$ HEVs (Figure 3C). In vitro, LFA-1–ICAM-1 engagements between transmigrated T cells and endothelial cells occur on the abluminal side,[35] raising the possibility that these interactions contributed to T-cell retention in the perivascular space observed here. Nonetheless, the perivascular dwelling time (8.0 ± 1.1 minute in WT PLNs vs 9.0 ± 1.1 minute in ICAM-1$^{-/-}$ PLNs), migration velocity, MI) and distance migrated were similar in the presence or absence of ICAM-1, suggesting that LFA-1–ICAM-1 interactions are not causing T-cell retention around HEVs after transmigration (Figure 3B-C). Once the cells left the perivascular region around ICAM-1–deficient HEVs, they showed increased directional persistence and speed (Figure 3C), albeit less so than T cells in ICAM-1–expressing lymph node stroma (supplemental Figure 6; supplemental Video 10), as previously observed.[16]

In summary, our data uncover a 3-step model of lymphocyte transmigration through HEVs, with ICAM-1–dependent intraluminal crawling in any direction as an optional first step. This is followed by the rapid crossing of the endothelial lining as a second step, which also occurs efficiently in the absence of ICAM-1. In a third step, T cells colocalizing with the basement membrane are retained in an ICAM-1–independent manner before entering the lymph node parenchyma and adopting their typical scanning behavior.

Successful T-cell transmigration across HEVs in the absence of ICAM-1 and ICAM-2

To further explore the contributions of endothelial ICAM-1, ICAM-2, or additional molecules for extravasation, we performed short-term in vivo homing assays where fluorescently labeled naive lymphocytes were injected intravenously into WT, ICAM-1$^{-/-}$, ICAM-2$^{-/-}$, and ICAM-1/2$^{-/-}$ mice. After 15, 30, or 60 minutes, PLNs were collected and analyzed by flow cytometry and immunohistology (Figure 4A). No significant difference in the absolute number of transferred lymphocytes was detected in ICAM-1 or ICAM-2 single-deficient PLNs (R.T.B., B.E., J.V.S., unpublished observations, 2009), despite the lower adhesiveness of ICAM-1$^{-/-}$ HEVs. Because blood-borne lymphocytes pass multiple times through HEV networks in the time course of a homing experiment, recirculating lymphocytes may eventually enter lymphoid tissue even in the absence of ICAM-1. On the other hand, transferred cells were reduced by 76% when both endothelial ICAM-1 and ICAM-2 were lacking (Figure 4B). All recovered T and B cells from WT and ICAM-1/2$^{-/-}$ PLNs were bona fide naive cells, as analyzed by CD62L and CD44 expression patterns (supplemental Figure 7).

In cryosections of WT PLNs, we observed a time-dependent increase in the absolute number of transferred lymphocytes (data not shown), as well as a shift in their localization over time. At 15 minutes after transfer, only a few cells were found outside the HEV basal membrane and inside the PLN parenchyma, while most transferred lymphocytes were associated with HEVs, that is, either intra- or perivascular (Figure 4C). The percentage of parenchymal cells increased over time such that 60 minutes after adoptive transfer, only 1 of 5 transferred cells was intra- or perivascular (Figure 4C). The appearance of adoptively transferred cells was not impaired in the absence of ICAM-1 or ICAM-2 alone. In contrast, in ICAM-1/2$^{-/-}$ PLNs twice as many lymphocytes were found to be still associated with HEVs compared with WT and ICAM-1– or

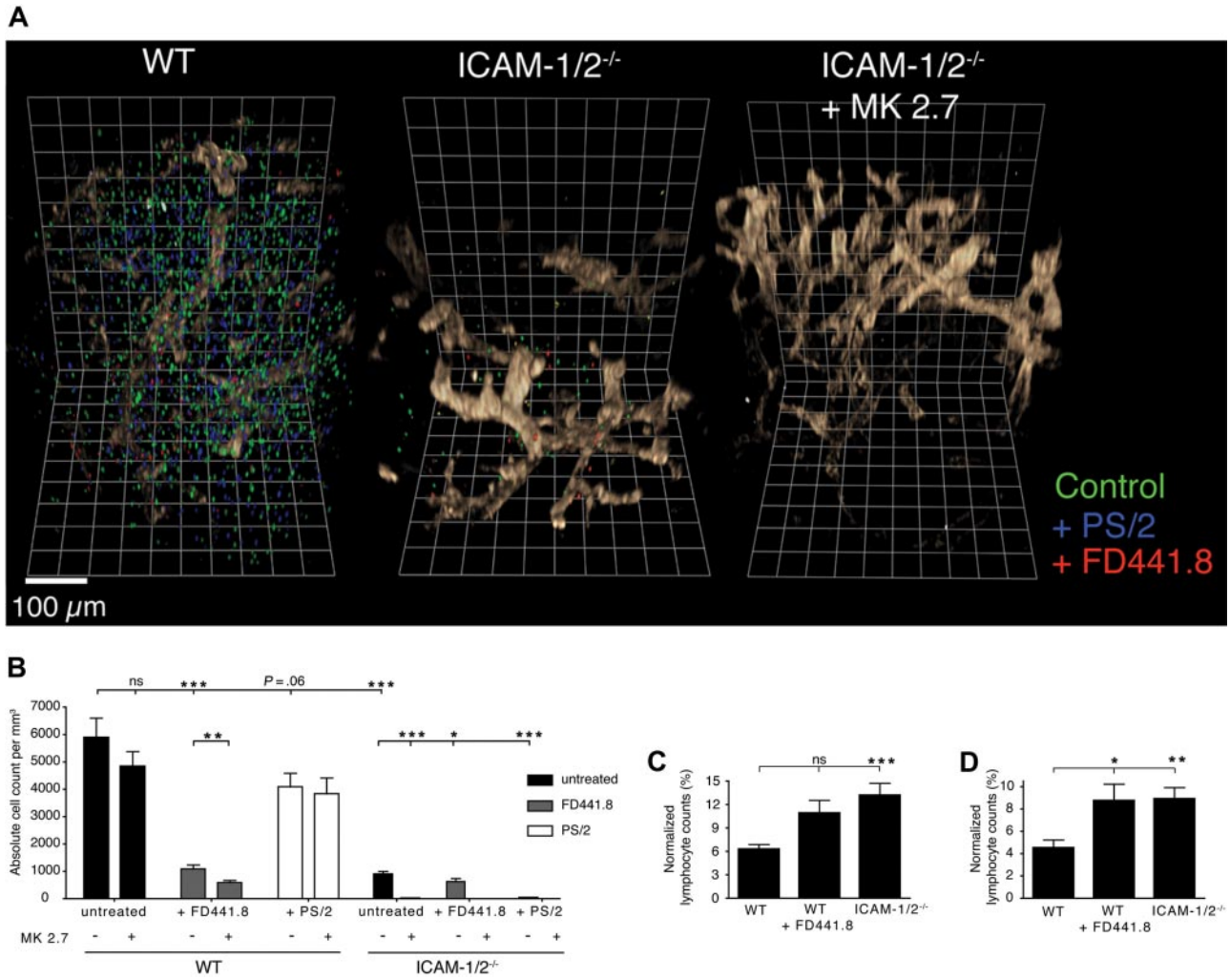

Figure 5. 3-dimensional quantitative immunofluorescence (3DQIF) of lymphocyte homing in the absence of ICAM-1, ICAM-2 and VCAM-1 during lymphocyte trafficking. (A) Representative 3D reconstructions of WT, ICAM-1/2$^{-/-}$, and ICAM-1/2$^{-/-}$ + anti–VCAM-1 mAb (MK2.7) PLNs after adoptive transfer of untreated lymphocytes (green), or treated with blocking anti–α4-integrin (PS/2, blue) or anti–LFA-1 (FD441.8, red). The MECA79^{+} HEV network is shown in brown. One square line corresponds to 50 μm. (B) Absolute cell counts per mm^3 in control and ICAM-1/2$^{-/-}$ PLNs in the presence of blocking mAbs. In some experiments, WT or ICAM-1/2$^{-/-}$ mice were pretreated with anti–VCAM-1 (MK2.7). Pooled from 5 experiments with 15 (ICAM-1/2$^{-/-}$) and 16 (WT) independent scans. (C) Intravascular frequency of adoptively transferred untreated lymphocytes in WT and ICAM-1/2$^{-/-}$ PLNs (right bar), and FD441.8-treated lymphocytes in WT PLNs (middle bar). (D) Perivascular frequency of adoptively transferred untreated lymphocytes in WT and ICAM-1/2$^{-/-}$ PLNs (right bar), and FD441.8-treated lymphocytes in WT PLNs (middle bar). Total cell counts in panels C and D were normalized to 100%. Data in panels C and D are pooled from 5 independent experiments. Bars represent mean plus minus SEM. n.s. indicates not significant. *$P < .05$; **$P < .001$; ***$P < .0001$.

ICAM-2–deficient mice. Interestingly, a significant number of lymphocytes was still able to cross HEVs and to enter the PLN parenchyma in the absence of ICAM-1 and ICAM-2 (Figure 4C).

3D immunofluorescence analysis of ICAM-1/2–dependent and –independent lymphocyte adhesion pathways in PLN HEVs

Our data suggested that both ICAM-1 and ICAM-2 were required for efficient lymphocyte homing, yet lymphocyte homing to ICAM-1/2$^{-/-}$ PLNs was not completely abolished. This observation prompted us to search for the identity of ICAM-1/2–independent lymphocyte homing mechanism to PLNs. In particular, we wanted to address whether α4- or additional LFA-1 integrin ligands were involved in homing. To circumvent the limitation of the very low detectable number of transferred lymphocytes per 2D section in the absence of both ICAMs, we developed 3-dimensional quantitative immunofluorescence (3DQIF; supplemental Figure 8). This approach enabled us to scan a large PLN volume and to increase the number of detected cells in WT and ICAM-1/2$^{-/-}$ PLNs to up to several thousand per scan (Figure 5A; supplemental Video 9). Furthermore, because the vasculature maintained its volume during processing, this approach allowed to clearly distinguishing intra- from perivascular cells (supplemental Figure 8). Using 3DQIF, we observed an 83% reduction in the absolute number of transferred lymphocytes in ICAM-1/2$^{-/-}$ PLNs after 60 minutes (Figure 5B). Lymphocyte pretreatment with anti–LFA-1 mAb caused only a minor decrease in the absolute cell number recovered from ICAM-1/2$^{-/-}$ PLNs, indicating that ICAM-independent LFA-1 ligands do not play a major role for lymphocyte adhesion. Blocking of α4-integrin alone caused no significant reduction of lymphocyte homing to WT PLNs, but almost completely inhibited lymphocyte homing to PLNs in mice lacking ICAM-1 and ICAM-2 (Figure 5B). Next, we performed 3DQIF after administration of anti–VCAM-1 mAbs 30 minutes before cell transfer. Blocking of endothelial VCAM-1 in ICAM-1/2$^{-/-}$ recipient mice efficiently abolished residual lymphocyte homing (Figure 5B). In WT recipient mice, blocking of endothelial VCAM-1 also caused a significant further reduction in homing of lymphocytes pretreated with anti–LFA-1 (Figure 5B), indicating that VCAM-1

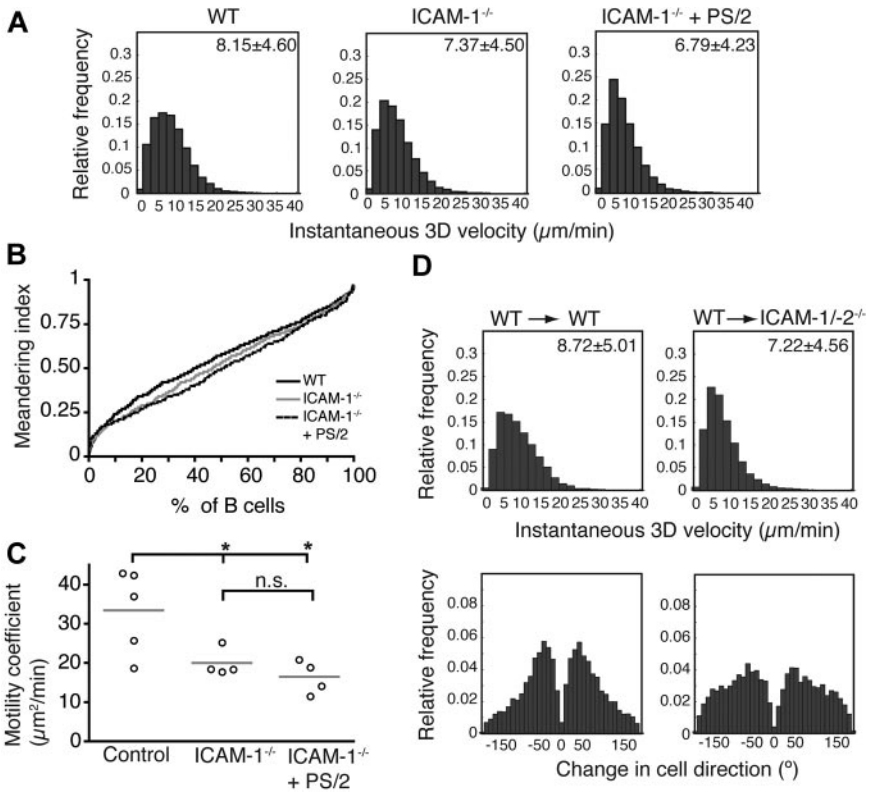

Figure 6. Follicular B-cell migration in absence of ICAM-1. (A) Instantaneous 3D velocity of follicular B cells in WT and ICAM-1$^{-/-}$ PLNs, treated or not with the anti-α4 blocking mAb PS/2. The mean velocity plus or minus SEM is indicated in the top right corner in μm/min. B cells are significantly slower in absence of ICAM-1 ($P < .001$), and their velocity can be further decreased after treatment with PS/2 ($P < .001$). (B) Normalized, cumulative meandering indices of B cells migrating in WT and ICAM-1$^{-/-}$ PLNs, treated or not with the anti-α4 blocking mAb PS/2. (C) Motility coefficients of B cells migrating in WT and ICAM-1$^{-/-}$ PLNs, treated or not with the anti-α4 blocking mAb PS/2. Absence of ICAM-1 significantly reduces the motility coefficient. n.s. indicates not significant. *$P < .05$. Data are pooled from 2 to 4 independent experiments yielding 4 to 5 image sequences containing 653, 345, and 340 cell tracks for WT, ICAM-1$^{-/-}$, and ICAM-1$^{-/-}$ + PS/2 PLNs, respectively. (D) Instantaneous 3D velocity (top panels) and change in cell direction distribution (turning angles, bottom panels) of follicular B cells in PLNs of WT and ICAM-1/-2$^{-/-}$ BM chimeras. For WT→WT BM chimera, 1 mouse per 4 image sequences per 442 cell tracks was analyzed, while for WT→ICAM-1-2$^{-/-}$ BM chimera, we examined 2 mice per 4 image sequences per 389 tracks.

is also present at low levels on the WT PLN microvasculature. Genetic deletion of both ICAM-1 and ICAM-2 or blocking of LFA-1 led to a slight yet significant reduction in the percentage of lymphocytes present in the PLN parenchyma, and a concomitant increase in intra- and perivascular cells (Figure 5C-D).

Thus, transmigration of transferred lymphocytes is only mildly impaired in the absence of ICAM-1 and ICAM-2, although overall homing is strongly reduced due to low adhesion in HEV. VCAM-1 is an alternative adhesion ligand, and perhaps also involved in the subsequent transmigration step.

ICAM-1 contributes to follicular B-cell motility

To examine whether follicular B-cell motility was affected by the absence of ICAM-1 and/or VCAM-1, we adoptively transferred B cells into WT and ICAM-1$^{-/-}$ recipients and performed 2PM analysis of their interstitial migration. Similar to observations in T cells (supplemental Figure 6; supplemental Videos 10-11), ICAM-1 deficiency caused a minor yet significant decrease of the migration velocity of B cells (Figure 6A; supplemental Videos 12-13). Treatment with blocking α4-integrin mAbs further caused a mild reduction in B-cell migration velocity and the accumulative MI as a measure for directional persistence ICAM-1$^{-/-}$ hosts (Figure 6A-B; supplemental Video 14). Nonetheless, absence of ICAM-1 alone resulted in a significantly lower motility coefficient compared with WT PLN (Figure 6C), whereas additional inhibition of α4 integrin caused no further decrease. Similarly, the motility of T and B cells in ICAM-1/-2$^{-/-}$-deficient PLNs in mice treated with the anti-α4 integrin mAb PS/2 was comparable with ICAM-1$^{-/-}$ PLNs (instantaneous 3D velocity for T cells 12.61 ± 9.50 μm/min and for B cells 6.75 μm/min ± 4.96 μm/min; pooled from 2 mice/4 image sequences/1709 tracks and 2/3/633 tracks, respectively; supplemental Video 15).

To examine whether ICAM-1 on hematopoietic cells contributed to parenchymal B-cell motility, we generated bone marrow (BM) chimeras in which WT BM cells were allowed to reconstitute the hematopoietic compartment in WT and ICAM-1/-2$^{-/-}$ mice. Adoptively transferred B cells showed a migration velocity decrease in the ICAM-1/-2$^{-/-}$ parenchyma of reconstituted mice similar to ICAM-1- or ICAM-1/-2-deficient PLNs (Figure 6D), indicating that ICAM-1 or ICAM-2 on hematopoietic cells do not contribute to parenchymal B-cell migration. Further blocking of α4 integrin activity did not further reduce B-cell motility in ICAM-1-2$^{-/-}$ BM chimeras (data not shown). The increased turning angle in ICAM-1/-2$^{-/-}$ BM chimeras indicated less directionality (Figure 6D), perhaps because of reduced guidance by stromal structures.

As a conclusion, stromal ICAM-1 contributes to follicular B-cell motility and directional persistence, while ICAM-2, VCAM-1, or MAdCAM-1 do not significantly enhance the scanning behavior of parenchymal B cells under homeostatic conditions.

Discussion

Lymphocyte maneuvering into and within lymphoid tissue requires transient adhesive interactions with stromal cells. Here, we performed an in-depth analysis of the contribution of the major Ig superfamily members expressed on these cells for efficient T- and B-cell trafficking. We used both genetic and mAb-blocking approaches to interfere with the lymphocyte's ability to bind ICAM-1, ICAM-2, and the α4 integrin ligands VCAM-1 and MAdCAM-1 on PLN endothelium and stroma cells. We found that ICAM-1 plays a dominant role for shear-resistant adhesion and intraluminal crawling, yet adhesion can also be mediated by ICAM-2, and to a low extent, by VCAM-1. Blocking all 3 molecules completely abolished lymphocyte adhesion within PLN HEVs. The kinetics of transmigration and perivascular trapping occurred comparably in the presence or absence of ICAM-1, while additional blocking of

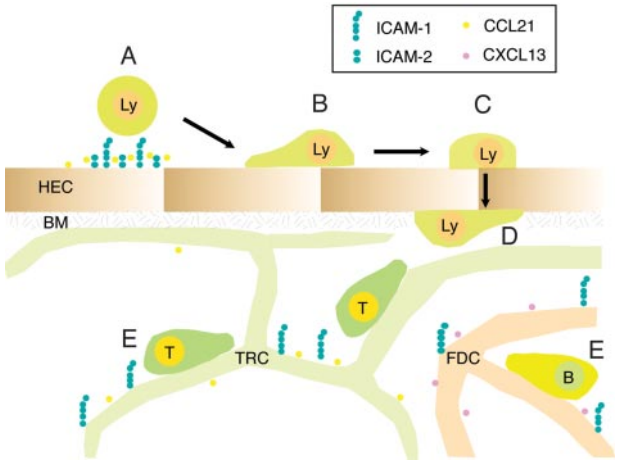

Figure 7. Proposed role for ICAM-1 and ICAM-2 during lymphocyte trafficking to and within PLNs. Blood-borne lymphocytes undergo rapid firm arrest in a largely ICAM-1 and ICAM-2-dependent manner, with a residual contribution of VCAM-1, in particular in the smallest HEVs (A). Approximately one-third of adherent T cells subsequently crawl on the luminal HEV surface, independent of the direction of the blood flow, in an ICAM-1-dependent manner (B). The rapid transmigration event (~ 1.5 minutes) can occur in the absence of endothelial ICAM-1 and ICAM-2 (C), and is followed in the majority of cells by "perivascular trapping" of the cells, perhaps because of entanglement with the basement membrane underlying the HEV and due to the cuff of surrounding fibroblastic stromal cells (D). Parenchymal ICAM-1 supports T- and B-cell motility through increased speed and directionality, presumably by allowing loose anchorage of scanning lymphocytes to the stromal network for guidance. Lymphocyte motility driven through chemokines and other factors can nonetheless take place efficiently in absence of ICAM-1 and α4 integrin ligands (E). HEC indicates high endothelial cell; BM, basement membrane; TRC, T-cell reticular zone cell; and FDC, follicular dendritic cell.

ICAM-2 caused a significant delay of lymphocyte accumulation in the lymphoid parenchyma. Crawling but not transmigration depended on cytoskeletal rearrangements through DOCK2-Rac activity. Finally, ICAM-1, but not ICAM-2 or the α4 integrin ligands VCAM-1 and/or MAdCAM-1, contributed to T- and B-cell scanning efficiency on follicular stromal cells (Figure 7).

Previous studies by Hamann and colleagues using homing assays have uncovered redundancy for ICAM-1 and ICAM-2 during lymphocyte accumulation in PLNs.[22] Genetic models and mAb blocking studies showed an essential role for LFA-1 during firm arrest of rolling lymphocytes inside HEVs.[10,36] In line with these observations, we found that shear-resistant lymphocyte adhesion was strongly reduced in ICAM-1/2$^{-/-}$ PLNs. MLN and PPs were also reduced in their cellularity, although the decrease was less strong presumably due to the expression of the alternative integrin ligand MAdCAM-1. LFA-1 inhibition did not further reduce lymphocyte adhesion in the absence of ICAM-1 and ICAM-2, indicating that no other LFA-1 ligands are involved in lymphocyte homing. Rather, residual homing was dependent on VCAM-1. Because we did not detect intraluminal lymphocytes in 3DQIF-reconstructed PLNs, we conclude that VCAM-1 directly participates in shear-resistant firm arrest. This likely occurs in highly adhesive HEVs with small diameter, as our IVM analysis suggests. Thus, although additional LFA-1– and α4-binding Ig superfamily members, such as JAM-A and JAM-B,[37,38] are present on HEVs, these molecules appear not to participate during shear-resistant adhesion. The reasons for this are currently unclear, but it is nonetheless conceivable that JAM family members play a supportive role during postadhesion events, such as transmigration, or during inflammation.

The observation that reduced lymphocyte homing to PLNs does not increase splenocyte numbers in ICAM-1/2$^{-/-}$ mice, despite a less stringent requirement for ICAMs in lymphocyte accumulation in the spleen, could be due to a direct role for integrin outside-in signaling for long-term survival of lymphocytes, or indirectly through reduced access to IL7-producing stromal cells found in lymph node tissue, but not in spleen.[39]

Intraluminal crawling of neutrophils, NK T cells, monocytes and lymphocytes have been observed in vivo as an additional step during leukocyte trafficking.[35,40-42] Our data assign a nonredundant role to ICAM-1 during the crawling step, thus serving as a "scanning molecule," while ICAM-2 appears to act uniquely during firm adhesion and perhaps transmigration. A similar preference for ICAM-1 over ICAM-2 was observed for intraluminal neutrophils, although these cells use Mac-1, rather than LFA-1, for crawling in cremaster muscle venules.[40] It is currently unclear whether crawling is required to reach an egress site, such as an endothelial junction, or whether cells can undergo both para- and transcellular transmigration.[43] It will be interesting to examine whether the intrinsic basic crawling capability of naive lymphocytes may be more pronounced after activation, because effector memory T cells may use luminal scanning of peripheral blood vessels for efficient immune surveillance.

ICAM-1 and VCAM-1 play an essential role during leukocyte transmigration through endothelial cells in vitro.[12-14] Unexpectedly, although transmigration efficiency was delayed in the absence of both ICAM-1 and ICAM-2, around 75% of adoptively transferred T cells in ICAM-1/2$^{-/-}$ PLNs still managed to enter the lymphoid parenchyma in short-term homing assays. It is unclear at the moment whether VCAM-1 forms a hypothetical "docking/transmigratory cup" in the absence of endothelial ICAMs, and which may then be required for successful transmigration. Alternatively, adherent lymphocytes, through engagement of their α4- or β2-integrins, may form probing filopodia as a prerequisite for transmigration, even in the absence of specialized Ig superfamily-containing structures on HEVs. This model does obviously not exclude the formation of ICAM-1-, ICAM-2- and VCAM-1-containing specialized docking/transmigration structures on WT HEVs. In cremaster muscle blood vessels, neutrophil egress is stepwise regulated by ICAM-2, JAM-A and PECAM-1.[44] Future studies need to analyze in more detail the precise requirements for ICAM-1, ICAM-2, VCAM-1 and other Ig superfamily members during effector lymphocyte egress within different microvascular beds.

Transmigrated T cells remained transiently attached to the abluminal side of HEVs, during which they actively probed the environment and frequently changed directionality, perhaps also influenced by high local chemokine concentrations.[45] The scanning behavior is compatible with an active path finding through the basement membrane, and/or by looking for gaps in the surrounding TRC cuff. In contrast, in in vitro flow assays, where cultured endothelial cells have a much reduced basement membrane thickness and no accessory cells are present, transmigrated naive lymphocytes show immediate high directional motility on the abluminal side[34] (data not shown), despite continuous LFA-1–ICAM-1 interactions.[35] Together with the notion that ICAM-1 is not causing a shorter perivascular dwelling time in HEVs, we conclude that lymphocyte retention on the abluminal side of HEVs is ICAM-1–independent, and may be rather due to mechanical trapping. Such retention could lead to an increased likelihood of T-cell–DC encounters during inflammation, as Ag-loaded DCs accumulate around HEVs.[46,47] Once moving along stromal networks in the T-cell area or B-cell follicles, ICAM-1 but not α4 integrin ligands contributes to efficient mouse T-cell motility,[16]

in contrast to recent in vitro observations with human T cells.[26] Similarly, B cells show a lower motility on ICAM-1$^{-/-}$ FDCs and MRCs, suggesting similar molecular mechanisms guiding parenchymal motility of both cell types. In fact, recent observations support a common migration mode of hematopoietic cells relying less on integrin-mediated adhesive interactions and more on lamellipodia-driven amoeboid motility in low-shear 3D networks.[48,49] This is contrasting with the ICAM-1–dependent migration on 2D surfaces we report here in vitro and in vivo, and likely reflects the different requirement for creating traction force in both circumstances.

To summarize, our data support a model in which Ig superfamily members, in particular ICAM-1 and ICAM-2, play a central role as anchorage proteins for shear-resistant firm arrest of lymphocytes in HEVs. Polarized intraluminal T cells crawl on ICAM-1; nonetheless, neither crawling nor presence of endothelial ICAM-1 was required for successful transmigration through PLN HEVs. Similarly, ICAM-1 on stromal cells increases the scanning efficiency, yet T and B cells still show considerable motility in the absence of ICAM-1. Homeostatic lymphocyte numbers within PLNs are achieved through carefully balanced T- and B-cell arrest and transmigration through HEV, followed by an inflammation-dependent dwelling time within the lymph node and egress via efferent lymphatics. Our data show that ICAM-1/2 deficiency affects mostly the very first step, that is, shear-resistant arrest, whereas the remaining steps are less affected.

Acknowledgments

We thank Pascal Halbherr, Miroslav Hons, and Varsha Kumar for help with experiments.

This work was supported by Swiss National Foundation grants SNF31-107510, 31-120640, and EU-MEXT 25405 (J.V.S.), and the Swiss National Foundation grant SNF3100A0-118390 (B.E.), the Swiss Multiple Sclerosis Society (B.E. and R.T.B.), and the National Multiple Sclerosis Society (B.E.).

Authorship

Contribution: R.T.B., F.P., K.G., A.I.C.S., A.M.M., S.F.S., D.N., and J.V.S. performed in vivo and in vitro experiments; S.H. and U.H.v.A. provided analysis software; Y.F. and U.D. provided vital material; M.M., B.E., and J.V.S. supervised the work and designed experiments; and R.T.B., B.E., and J.V.S. wrote the manuscript.

Conflict-of-interest disclosure The authors declare no competing financial interests.

Correspondence: Britta Engelhardt, University of Bern, Theodor Kocher Institute, Freiestrasse 1, 3012 Bern, Switzerland; e-mail: bengel@tki.unibe.ch; and Jens V. Stein, University of Bern, Theodor Kocher Institute, Freiestrasse 1, 3012 Bern, Switzerland; e-mail: jstein@tki.unibe.ch.

References

1. Junt T, Scandella E, Ludewig B. Form follows function: lymphoid tissue microarchitecture in antimicrobial immune defence. *Nat Rev Immunol.* 2008;8(10):764-775.
2. Cyster JG. Chemokines, sphingosine-1-phosphate, and cell migration in secondary lymphoid organs. *Annu Rev Immunol.* 2005;23127-159.
3. von Andrian UH, Mempel TR. Homing and cellular traffic in lymph nodes. *Nat Rev Immunol.* 2003;3(11):867-878.
4. Bajénoff M, Glaichenhaus N, Germain RN. Fibroblastic reticular cells guide T lymphocyte entry into and migration within the splenic T cell zone. *J Immunol.* 2008;181(6):3947-3954.
5. Katakai T, Suto H, Sugai M, et al. Organizer-like reticular stromal cell layer common to adult secondary lymphoid organs. *J Immunol.* 2008; 181(9):6189-6200.
6. Link A, Vogt TK, Favre S, et al. Fibroblastic reticular cells in lymph nodes regulate the homeostasis of naive T cells. *Nat Immunol.* 2007;8(11):1255-1265.
7. Stein JV, Rot A, Luo Y, et al. The CC chemokine thymus-derived chemotactic agent 4 (TCA-4, secondary lymphoid tissue chemokine, 6Ckine, exodus-2) triggers lymphocyte function-associated antigen 1-mediated arrest of rolling T lymphocytes in peripheral lymph node high endothelial venules. *J Exp Med.* 2000;191(1):61-76.
8. Baekkevold ES, Yamanaka T, Palframan RT, et al. The CCR7 ligand elc (CCL19) is transcytosed in high endothelial venules and mediates T cell recruitment. *J Exp Med.* 2001;193(9):1105-1112.
9. Alon R, Dustin ML. Force as a facilitator of integrin conformational changes during leukocyte arrest on blood vessels and antigen-presenting cells. *Immunity.* 2007;26(1):17-27.
10. Warnock RA, Askari S, Butcher EC, von Andrian UH. Molecular mechanisms of lymphocyte homing to peripheral lymph nodes. *J Exp Med.* 1998; 187(2):205-216.
11. Shamri R, Grabovsky V, Gauguet JM, et al. Lymphocyte arrest requires instantaneous induction of an extended LFA-1 conformation mediated by endothelium-bound chemokines. *Nat Immunol.* 2005;6(5):497-506.
12. Carman CV, Springer TA. Trans-cellular migration: cell-cell contacts get intimate. *Curr Opin Cell Biol.* 2008;20(5):533-540.
13. Carman CV, Springer TA. A transmigratory cup in leukocyte diapedesis both through individual vascular endothelial cells and between them. *J Cell Biol.* 2004;167(2):377-388.
14. Barreiro O, Yanez-Mo M, Serrador JM, et al. Dynamic interaction of VCAM-1 and ICAM-1 with moesin and ezrin in a novel endothelial docking structure for adherent leukocytes. *J Cell Biol.* 2002;157(7):1233-1245.
15. Bajénoff M, Egen JG, Koo LY, et al. Stromal cell networks regulate lymphocyte entry, migration, and territoriality in lymph nodes. *Immunity.* 2006; 25(6):989-1001.
16. Woolf E, Grigorova I, Sagiv A, et al. Lymph node chemokines promote sustained T lymphocyte motility without triggering stable integrin adhesiveness in the absence of shear forces. *Nat Immunol.* 2007;8(10):1076-1085.
17. Lammermann T, Bader BL, Monkley SJ, et al. Rapid leukocyte migration by integrin-independent flowing and squeezing. *Nature.* 2008;453(7191):51-55.
18. Nombela-Arrieta C, Mempel TR, Soriano SF, et al. A central role for DOCK2 during interstitial lymphocyte motility and sphingosine-1-phosphate-mediated egress. *J Exp Med.* 2007;204(3):497-510.
19. Maeda K, Kosco-Vilbois MH, Burton GF, Szakal AK, Tew JG. Expression of the intercellular adhesion molecule-1 on high endothelial venules and on non-lymphoid antigen handling cells: interdigitating cells, antigen transporting cells and follicular dendritic cells. *Cell Tissue Res.* 1995;279(1): 47-54.
20. Constantin G, Majeed M, Giagulli C, et al. Chemokines trigger immediate beta2 integrin affinity and mobility changes: differential regulation and roles in lymphocyte arrest under flow. *Immunity.* 2000;13(6):759-769.
21. Baekkevold ES, Jahnsen FL, Johansen FE, et al. Culture characterization of differentiated high endothelial venule cells from human tonsils. *Lab Invest.* 1999;79(3):327-336.
22. Lehmann JC, Jablonski-Westrich D, Haubold U, Gutierrez-Ramos JC, Springer T, Hamann A. Overlapping and selective roles of endothelial intercellular adhesion molecule-1 (ICAM-1) and ICAM-2 in lymphocyte trafficking. *J Immunol.* 2003;171(5):2588-2593.
23. Berlin-Rufenach C, Otto F, Mathies M, et al. Lymphocyte migration in lymphocyte function-associated antigen (LFA)-1-deficient mice. *J Exp Med.* 1999;189(9):1467-1478.
24. Szabo MC, Butcher EC, McEvoy LM. Specialization of mucosal follicular dendritic cells revealed by mucosal addressin-cell adhesion molecule-1 display. *J Immunol.* 1997;158(12):5584-5588.
25. Lo CG, Lu TT, Cyster JG. Integrin-dependence of Lymphocyte Entry into the Splenic White Pulp. *J Exp Med.* 2003;197(3):353-361.
26. Hyun YM, Chung HL, McGrath JL, Waugh RE, Kim M. Activated integrin VLA-4 localizes to the lamellipodia and mediates T cell migration on VCAM-1. *J Immunol.* 2009;183(1):359-369.
27. Xu H, Gonzalo JA, St Pierre Y, et al. Leukocytosis and resistance to septic shock in intercellular adhesion molecule 1-deficient mice. *J Exp Med.* 1994;180(1):95-109.
28. Gerwin N, Gonzalo JA, Lloyd C, et al. Prolonged eosinophil accumulation in allergic lung interstitium of ICAM-2 deficient mice results in extended hyperresponsiveness. *Immunity.* 1999;10(1):9-19.
29. Lyck R, Reiss Y, Gerwin N, Greenwood J, Adamson P, Engelhardt B. T-cell interaction with ICAM-1/ICAM-2 double-deficient brain endothelium in vitro: the cytoplasmic tail of endothelial ICAM-1 is necessary for transendothelial migration of T cells. *Blood.* 2003;102(10):3675-3683.

30. von Andrian UH. Intravital microscopy of the peripheral lymph node microcirculation in mice. *Microcirculation.* 1996;3(3):287-300.
31. Mempel TR, Henrickson SE, Von Andrian UH. T-cell priming by dendritic cells in lymph nodes occurs in three distinct phases. *Nature.* 2004;427 (6970):154-159.
32. Fukui Y, Hashimoto O, Sanui T, et al. Haematopoietic cell-specific CDM family protein DOCK2 is essential for lymphocyte migration. *Nature.* 2001; 412(6849):826-831.
33. Nombela-Arrieta C, Lacalle RA, Montoya MC, et al. Differential Requirements for DOCK2 and Phosphoinositide-3-Kinase gamma during T and B Lymphocyte Homing. *Immunity.* 2004;21(3): 429-441.
34. Shulman Z, Pasvolsky R, Woolf E, et al. DOCK2 regulates chemokine-triggered lateral lymphocyte motility but not transendothelial migration. *Blood.* 2006;108(7):2150-2158.
35. Shulman Z, Shinder V, Klein E, et al. Lymphocyte crawling and transendothelial migration require chemokine triggering of high-affinity LFA-1 integrin. *Immunity.* 2009;30(3):384-396.
36. Hamann A, Jablonski-Westrich D, Duijvestijn A, et al. Evidence for an accessory role of LFA-1 in lymphocyte-high endothelium interaction during homing. *J Immunol.* 1988;140(3):693-699.
37. Pfeiffer F, Kumar V, Butz S, et al. Distinct molecular composition of blood and lymphatic vascular endothelial cell junctions establishes specific functional barriers within the peripheral lymph node. *Eur J Immunol.* 2008;38(8):2142-2155.
38. Weber C, Fraemohs L, Dejana E. The role of junctional adhesion molecules in vascular inflammation. *Nat Rev Immunol.* 2007;7(6):467-477.
39. Repass JF, Laurent MN, Carter C, et al. IL7-hCD25 and IL7-Cre BAC transgenic mouse lines: new tools for analysis of IL-7 expressing cells. *Genesis.* 2009;47(4):281-287.
40. Phillipson M, Heit B, Colarusso P, Liu L, Ballantyne CM, Kubes P. Intraluminal crawling of neutrophils to emigration sites: a molecularly distinct process from adhesion in the recruitment cascade. *J Exp Med.* 2006;203(12):2569-2575.
41. Auffray C, Fogg D, Garfa M, et al. Monitoring of blood vessels and tissues by a population of monocytes with patrolling behavior. *Science.* 2007;317(5838):666-670.
42. Geissmann F, Cameron TO, Sidobre S, et al. Intravascular immune surveillance by CXCR6+ NKT cells patrolling liver sinusoids. *PLoS Biol.* 2005;3(4):e113.
43. Engelhardt B, Wolburg H. Mini-review: Transendothelial migration of leukocytes: through the front door or around the side of the house? *Eur J Immunol.* 2004;34(11):2955-2963.
44. Woodfin A, Voisin MB, Imhof BA, Dejana E, Engelhardt B, Nourshargh S. Endothelial cell activation leads to neutrophil transmigration as supported by the sequential roles of ICAM-2, JAM-A, and PECAM-1. *Blood.* 2009;113(24): 6246-6257.
45. Miyasaka M, Tanaka T. Lymphocyte trafficking across high endothelial venules: dogmas and enigmas. *Nat Rev Immunol.* 2004;4(5): 360-370.
46. Bajénoff M, Granjeaud S, Guerder S. The strategy of T cell antigen-presenting cell encounter in antigen-draining lymph nodes revealed by imaging of initial T cell activation. *J Exp Med.* 2003; 198(5):715-724.
47. Katakai T, Hara T, Lee JH, Gonda H, Sugai M, Shimizu A. A novel reticular stromal structure in lymph node cortex: an immuno-platform for interactions among dendritic cells, T cells and B cells. *Int Immunol.* 2004;16(8):1133-1142.
48. Lammermann T, Sixt M. The microanatomy of T-cell responses. *Immunol Rev.* 2008;22126-22143.
49. Friedl P, Weigelin B. Interstitial leukocyte migration and immune function. *Nat Immunol.* 2008; 9(9):960-969.